PHYSICAL REVIEW D **90,** 095016 (2014)

Strongly interacting dark matter: Self-interactions and keV lines

Kimberly K. Boddy,[1] Jonathan L. Feng,[2,3] Manoj Kaplinghat,[2] Yael Shadmi,[4] and Timothy M. P. Tait[2]

[1]*Walter Burke Institute for Theoretical Physics, California Institute of Technology, Pasadena, California 91125, USA*

[2]*Department of Physics and Astronomy, University of California, Irvine, California 92697, USA*

[3]*CERN Theory Division, CH-1211 Geneva 23, Switzerland*

[4]*Physics Department, Technion—Israel Institute of Technology, Haifa 32000, Israel*

(Received 9 September 2014; published 18 November 2014)

We consider a simple supersymmetric hidden sector: pure SU(N) gauge theory. Dark matter is made up of hidden glueballinos with mass m_X and hidden glueballs with mass near the confinement scale Λ. For $m_X \sim 1$ TeV and $\Lambda \sim 100$ MeV, the glueballinos freeze out with the correct relic density and self-interact through glueball exchange to resolve small-scale structure puzzles. An immediate consequence is that the glueballino spectrum has a hyperfine splitting of order $\Lambda^2/m_X \sim 10$ keV. We show that the radiative decays of the excited state can explain the observed 3.5 keV x-ray line signal from clusters of galaxies, Andromeda, and the Milky Way.

DOI: 10.1103/PhysRevD.90.095016 PACS numbers: 95.35.+d, 12.60.Jv, 95.85.Nv

I. INTRODUCTION

The field of particle dark matter is at an interesting juncture. Direct, indirect, and collider searches for dark matter are improving rapidly, but have not yet yielded unambiguous signals. At the same time, the astrophysical evidence for dark matter with $\Omega_{\rm DM}h^2 = 0.1196 \pm 0.0031$ [1] remains as strong as ever, and there are now tantalizing astrophysical indications that dark matter may be self-interacting [2–5] or the source of an observed 3.5 keV x-ray line from galaxies and clusters of galaxies [6,7]. Self-interactions and the 3.5 keV line have each merited a great deal of attention, although typically separately, without any attempt to relate them in a simple framework.

Given the existing evidence for dark matter, a natural possibility is that dark matter is in a hidden sector, composed of particles with no standard model gauge interactions [8]. In general, hidden sectors are decoupled from most of particle physics, both in terms of their theoretical motivations and their testable predictions. In the framework of supersymmetry, however, hidden sectors may emerge from more fundamental theories and contain particles that have the desired thermal relic density through the WIMPless miracle [9–13]. Although much of our analysis below will be independent of supersymmetry, the possibility of preserving this fundamental feature of weakly-interacting massive particles is a significant virtue, and for concreteness, we will consider hidden sectors with supersymmetry.

Here we consider the simplest possible UV-complete supersymmetric hidden sector: a pure SU(N) gauge theory. This sector introduces only two new particles: gluons g and gluinos $\tilde{g}$, which hadronize into glueballs $G \equiv (gg)$ and glueballinos $\tilde{G} \equiv (\tilde{g}g)$. Throughout this work, references to color, gluons, gluinos, and their composite states refer to the hidden sector. For other work on strongly interacting dark matter, see Refs. [14–28].

We find that this simple hidden sector may explain all of the above-noted astrophysical observations. For gluino mass $m_X \sim$ TeV and glueball mass near the confinement scale $\Lambda \sim 100$ MeV, glueballinos have both the correct relic density and self-interaction cross section to resolve small-scale structure puzzles [25]. These considerations fix the glueballino spectrum's hyperfine splitting $\Delta E = m_{\tilde{G}^*} - m_{\tilde{G}} \sim \Lambda^2/m_X \sim 10$ keV. Introducing connector fields that couple the hidden and visible sectors, we find that radiative decays $\tilde{G}^* \to \tilde{G}\gamma$ may have the energy and flux required to explain the observed x-ray line signals in both "short lifetime" and "long lifetime" scenarios.

II. GLUEBALLINO RELIC DENSITY AND REANNIHILATION

The supersymmetric pure SU(N) hidden sector may be completely characterized by the four parameters

$$m_X, \qquad \Lambda, \qquad N, \qquad \xi_f, \tag{1}$$

which are the gluino mass, the confinement scale, the number of colors, and the ratio of hidden to visible sector temperatures at gluino freeze-out, respectively. In terms of these parameters, the fine-structure constant at the scale m_X is given by the renormalization group relation

$$\alpha_X = \frac{6\pi}{11N \ln(m_X/\Lambda)}. \tag{2}$$

Gluinos freeze out with relic density [10]

$$\Omega_{\tilde{g}} \approx \frac{s_0}{\rho_{c0}} \frac{\sqrt{g_*^{\rm tot}}}{g_{*S}(T_f)} \frac{3.79 x_f}{M_{\rm Pl}\langle\sigma v\rangle}, \tag{3}$$

where s_0 is the visible sector entropy today, ρ_{c0} is the critical density today, $g_{*S}(T_f)$ is the entropy effective number of degrees of freedom in the visible sector at freeze-out, $g_*^{\rm tot}(T_f) = g_*(T_f) + \xi_f^4 2(N^2-1)$, $M_{\rm Pl} \simeq 1.2 \times 10^{19}$ GeV, and $x_f \equiv m_X/T_f \approx 25\xi_f$. The gluinos annihilate through the S-wave process $\tilde{g}\tilde{g} \to gg$ with cross section

$$\langle \sigma v \rangle = \frac{3}{8}\frac{N^2}{N^2-1}\frac{\pi\alpha_X^2}{m_X^2}. \tag{4}$$

When the Universe cools to a temperature below Λ, the gluinos and gluons hadronize into glueballinos and glueballs. The glueballinos then interact with an enhanced geometric cross section $\sim\Lambda^{-2}$, which may initiate an era of reannihilation, depleting the gluino relic density. However, the glueballinos typically form in a state with high angular momentum L [14]. For the constituent gluinos to annihilate, this bound state must first decay to a low-L state by radiating glueballs. (Note that there are no hidden light pions or photons.) Reannihilation therefore requires $\alpha_X^2 m_X \gtrsim N_G \Lambda$, where N_G is the number of glueballs radiated. N_G is at least 1. More typically, it is the angular momentum of the bound state $N_G \sim L \sim m_X v r \sim m_X\sqrt{\Lambda/m_X}\Lambda^{-1}$. Below, we will therefore exclude regions where $\alpha_X^2 \gtrsim \sqrt{\Lambda/m_X}$, and reannihilation may be significant. Note that this constraint may be overly stringent, since glueballs will readily break apart high-L bound states.

III. GLUEBALL RELIC DENSITY AND CANNIBALIZATION

After gluinos freeze out, the gluons maintain thermal equilibrium. Upon confinement, the gluon energy density becomes the glueball energy density [25]

$$\Omega_G \approx \frac{s_0}{\rho_{c0}}\frac{2(N^2-1)}{g_{*S}(T_f)}\xi_f^3 \times \begin{cases} T_d^h & \text{for } T_d^h < \Lambda \\ \Lambda & \text{otherwise,} \end{cases} \tag{5}$$

where T_d^h is the hidden sector temperature at the time of chemical decoupling. Equation (5) may be understood as follows: In the absence of self-interactions, the glueballs decouple early, and the relic density is simply the thermal number density multiplied by the glueball mass $\sim\Lambda$. With significant self-interactions, however, the glueballs may remain in chemical equilibrium even after the temperature drops below Λ through, for example, $3 \to 2$ number-changing processes. This depletion of glueball number is referred to as cannibalization [29]. Eventually, the expansion of the Universe causes the glueballs to decouple at a temperature T_d^h, and entropy and glueball number conservation after decoupling imply that $\Omega_G \propto T_d^h$. We have numerically solved for the glueball density accounting for cannibalization, following Ref. [29], and find that cannibalization reduces Ω_G by less than a factor of 2 in the parameter range of interest.

It is also possible to eliminate the glueball relic density altogether by postulating additional interactions with the visible sector. For example, before confinement, gluons may annihilate to sterile neutrinos, which quickly decay to light visible sector particles before they can annihilate back into gluons [25]. We will consider cases in which the glueball relic density is given by Eq. (5), and also those in which glueballs are effectively absent.

IV. SELF-INTERACTIONS

Discrepancies between simulations and observations on small scales may be resolved if dark matter self-interacts with cross-section-to-mass ratio $\sigma/m \sim 1\ \text{cm}^2/\text{g} \sim 1\ \text{barn}/\text{GeV}$. To determine the self-interactions of glueballs and glueballinos, we follow the analysis of Ref. [25], which we summarize here.

For glueballs, we take the geometric cross section $\sigma_G = 4\pi/\Lambda^2$, which is of the desired size for $\Lambda \sim 100$ MeV.

Glueballino self-interactions are mediated by glueball exchange, which we model as an attractive Yukawa potential $V(r) = -e^{-\Lambda r}/r$. The self-interaction cross section $\sigma_{\tilde{G}}$ is $\langle\sigma_T\rangle$; the transfer cross section $\sigma_T = \int d\Omega(1-\cos\theta)\times(d\sigma/d\Omega)$, averaged over Maxwell-Boltzmann velocity distributions with characteristic velocities $v_0 = 40$, 100, and 1000 km/s for dwarf galaxies, low-surface-brightness spiral galaxies (LSBs), and clusters, respectively. For $m_X \sim$ TeV, $\Lambda \sim 10$ MeV gives the desired self-interactions.

The case of mixed glueballino-glueball dark matter is much more complicated. As a very simple measure in this general case, we define

$$\sigma/m = \frac{\sigma_{\tilde{G}}}{m_X}\frac{\Omega_{\tilde{G}}}{\Omega_{\rm DM}} + \frac{\sigma_G}{\Lambda}\frac{\Omega_G}{\Omega_{\rm DM}}, \tag{6}$$

which has the correct behavior in the limits of pure $\tilde{G}$ or pure G dark matter and interpolates between them.

V. GLUEBALLINO HYPERFINE STRUCTURE AND TRANSITIONS

There are two S-wave glueballino states: the spin-1/2 ground state $\tilde{G}$ and the spin-3/2 excited state $\tilde{G}^*$ [30]. In the case of atomic hydrogen, the hyperfine splitting created by the electromagnetic interactions is $\sim\alpha_{\rm EM}^4 m_e^2/m_p$. In the present case, we expect the hidden chromomagnetic interactions to yield hyperfine splittings

$$\Delta E = m_{\tilde{G}^*} - m_{\tilde{G}} = c_E \Lambda^2/m_X, \tag{7}$$

with $c_E \sim 1$ an order 1 coefficient that depends on the strong dynamics. Lattice results for the hyperfine splittings of B mesons [31] suggest $c_E \approx 5$ for those systems.

In the absence of other interactions, the $\tilde{G}^*$ state is stable. To make contact with the x-ray observations, we introduce a connector field with mass m_C and both hidden color and

visible electromagnetic quantum numbers. Dipole operators vanish, since the gluino is a Majorana fermion. But one-loop diagrams with virtual heavy connectors induce at leading order the Kähler potential term

$$c_\tau \frac{1}{m_C^3}\int d^4\theta W_\alpha^h W^\alpha \bar{D}^{\dot\alpha}\bar{W}_{\dot\alpha}^h \bar{S}. \quad (8)$$

This leads to the dimension-6 interaction

$$c_\tau \frac{m}{m_C^3}\bar{\tilde{g}}\gamma^\mu D^\nu \tilde{g} F_{\mu\nu}, \quad (9)$$

where W^h (W) is the hidden (visible) gauge superfield, F is the visible electromagnetic field strength, $\langle S\rangle = \tilde{m}\theta^2$ is a spurion representing the influence of supersymmetry breaking, and c_τ is a dimensionless coefficient, which we estimate to be $c_\tau \sim e\alpha_h/(4\pi)$. At the hadronic level, this mediates the decay $\tilde{G}^* \to \tilde{G}\gamma$ with lifetime

$$\tau \sim \frac{32\pi^2}{\alpha_{\rm EM}\alpha_h^2}\frac{m_C^6}{\tilde{m}^2\Lambda^2\Delta E^3} \sim 6.2\times 10^{14}\ {\rm s} \times \left[\frac{0.01}{\alpha_h}\right]^2\left[\frac{m_C}{\rm TeV}\right]^6\left[\frac{\rm TeV}{\tilde{m}}\right]^2\left[\frac{100\ {\rm MeV}}{\Lambda}\right]^2\left[\frac{3.5\ {\rm keV}}{\Delta E}\right]^3, \quad (10)$$

where $m_X \lesssim \tilde{m} \lesssim m_C$. Decays to neutrinos or multiple photons are also possible, but will be suppressed by additional powers of m_C and phase space.

VI. THE 3.5 KEV LINE

The stacked XMM-Newton spectrum of 73 clusters of galaxies has revealed a weak x-ray line at 3.55–3.57 keV [6]. The line is also seen in the Perseus cluster by both XMM-Newton and Chandra [6,7], in the stacking of Centaurus, Ophiuchus and Coma, and in the stacking of all clusters except these four [6]. A line close to this energy is also seen towards the Andromeda galaxy (M31) [7] and the center of the Milky Way (MW) [32]. The measured fluxes by XMM-Newton from Perseus (without the core), M31, and the MW are shown in Table I. The initial analyses have motivated a great deal of follow-up activity, including supporting evidence, null results, and proposed explanations in terms of line emission from ions [33–37].

TABLE I. 3.5 keV line fluxes and cored halo parameters.

	Flux (10^{-6} cm^{-2} s^{-1})	J (kpc GeV^2/cm^6)	Σ (kpc GeV/cm^3)
Perseus	$21.4^{+7.0}_{-6.3}$ [6]	2.3	20
M31	$4.9^{+1.6}_{-1.3}$ [7]	8.2	13
MW	29 ± 5 [32]	41	37

Here we consider the possibility that this line is a signal from the deexcitation of dark matter.[1] There are two limiting scenarios. In the short-lifetime scenario, the $\tilde{G}^*$ lifetime is $\tau \lesssim 10^{15}$ s. $\tilde{G}^*$ states are created in inelastic collisions $\tilde{G}\tilde{G} \to \tilde{G}\tilde{G}^*$ and then decay. The signal is a dark matter analogue to the 21 cm line of neutral hydrogen [39–41] and is proportional to ρ^2, where ρ is the dark matter mass density. The predicted flux is

$$F_{\rm short} = \frac{\langle\sigma_{\tilde{G}^*}v\rangle}{8\pi m_X^2}\left\langle\int \rho^2 d\ell\right\rangle_{\rm FOV} = \frac{1.1\times 10^{-3}}{\rm cm^2\ s}\left[\frac{\rm TeV}{m_X}\right]\left[\frac{\langle\sigma_{\tilde{G}^*}v/c\rangle/m_X}{10^{-3}\ {\rm barn/GeV}}\right] \times \left[\frac{J}{\rm kpc\ GeV^2/cm^6}\right]\left[\frac{\rm FOV}{\rm deg^2}\right], \quad (11)$$

where the integral is along the line of sight, FOV is the field of view of the measurement, $J \equiv \langle\int \rho^2 d\ell\rangle_{\rm FOV}$ is an average over this FOV, and $\sigma_{\tilde{G}^*} = \sigma(\tilde{G}\tilde{G} \to \tilde{G}\tilde{G}^*)$ is the cross section for creating excited states $\tilde{G}^*$. For $m_X \sim$ TeV, the kinetic energy in $\tilde{G}\tilde{G}$ scattering is typically large compared to the hyperfine splitting. We therefore expect the inelastic and elastic cross sections to be similar to each other and to the transfer cross section, as is the case in an atomic dark matter model [42]. It is tantalizing that the indicated cross sections from self-interactions and the 3.5 keV line are roughly similar, despite their being completely disparate phenomena.

Before we determine what values of $\sigma_{\tilde{G}^*}$ are favored, however, we must ask if *any* value of $\sigma_{\tilde{G}^*}$ can explain all the data. To do this, we must determine J for halo profiles that are consistent with self-interacting dark matter and compare them to the observed fluxes. For the MW and M31, the FOV is a cone with a 14' half-angle. The MW observations are centered on the Galactic center. The equilibrium self-interacting dark matter solution [43] requires that the core radius be set by the gravitational potential of the stars, since they dominate at the center. We use a modified Navarro-Frenk-White profile, $\rho(r) \propto 1/(r+r_c)/(r+r_s)^2$ with $r_s = 21$ kpc and core radius $r_c = 0.5$ kpc, normalized to a local density of 0.4 GeV/cm^3 [43]. For M31, we use a similar profile, but with a density at 8.5 kpc of 0.2 GeV/cm^3. For Perseus, we compute the flux in a projected radius of 240 kpc using $M_{\rm vir} = 1.1\times 10^{15} M_\odot$ and a concentration parameter $R_{\rm vir}/r_s = 6$, which gives rise to the same surface density within 240 kpc as that in Ref. [6]. The resulting J values are given in Table I.

Equation (11) and the J and flux values of Table I imply

$$\frac{\sigma_{\tilde{G}^*}}{m_X} \sim 0.016(0.005)[0.006]\ \frac{\rm barn}{\rm GeV}\left[\frac{m_X}{\rm TeV}\right]\left[\frac{\Omega_{\rm DM}}{\Omega_{\tilde{G}}}\right]^2, \quad (12)$$

[1] For other alternatives, see e.g., [38].

for Perseus (M31) [MW]. Taken at face value, these results are in tension because we expect $\sigma_{\tilde{G}^*}$ to follow $\sigma_{\tilde{G}}$ and be smaller in the clusters due to the larger relative velocities. At the same time, there are considerable uncertainties from halo modeling [40] and line flux measurements. Below, we focus on Perseus for the short-lifetime scenario, keeping this tension in mind.

Dwarf spheroidal satellite galaxies of the Milky Way constrain the short-lifetime scenario. For most dwarfs, we expect $J \gtrsim (0.1 M_\odot/\mathrm{pc}^3)^2 \times 0.6\ \mathrm{kpc} \sim 10\ \mathrm{kpc\,GeV^2/cm^6}$, using the observed commonality of halo masses within 300 pc [44]. Using $v/c \sim 10^{-4}$ and $\sigma_{\tilde{G}^*}/m_X = 0.01\ \mathrm{barn/GeV}$, we predict a flux of $2 \times 10^{-6}/\mathrm{cm^2\,s}$, about an order of magnitude larger than the stacked dwarf limit [35]. However, for dwarfs and $m_X \sim$ 100 GeV–1 TeV, the kinetic energy of the collision satisfies $m_X v^2/2 \lesssim \Delta E$, and so a detailed analysis of $\sigma_{\tilde{G}^*}$ is required to predict the flux from dwarfs.

Alternatively, in the long-lifetime scenario, the $\tilde{G}^*$ lifetime is longer than the age of the Universe, $\tau \gtrsim 10^{18}$ s. The $\tilde{G}^*$ states are created at the time of hadronization, and since the hyperfine splitting is small compared to the temperature at confinement, the number densities of $\tilde{G}$ and $\tilde{G}^*$ are identical at that time. The $\tilde{G}^*$ states then slowly decay, with a signal proportional to ρ and flux

$$F_{\mathrm{long}} = \frac{1}{4\pi m_X \tau}\left\langle \int \rho\, d\ell \right\rangle_{\mathrm{FOV}} \mathrm{FOV} = \frac{7.5\times 10^{-7}}{\mathrm{cm^2\,s}}\left[\frac{\mathrm{TeV}}{m_X}\right]\left[\frac{10^{20}\ \mathrm{s}}{\tau}\right]\left[\frac{\Sigma}{\mathrm{kpc\,GeV/cm^3}}\right]\left[\frac{\mathrm{FOV}}{\mathrm{deg^2}}\right], \quad (13)$$

where $\Sigma = \langle \int \rho\, d\ell \rangle_{\mathrm{FOV}}$ is the surface density. Values of Σ for the halo models described above are given in Table I.

Equation (13) and the Σ and flux values of Table I imply

$$\tau \sim 200(500)[300]\ \mathrm{Gyr}\left[\frac{\mathrm{TeV}}{m_X}\right]\left[\frac{\Omega_{\tilde{G}^*}}{\frac{1}{2}\Omega_{\mathrm{DM}}}\right], \quad (14)$$

for Perseus (M31) [MW]. Given the large systematic uncertainties in the M31 measurement [7], these three signals are consistent in the long-lifetime scenario.

We have checked that the required lifetimes are not in conflict with cosmic microwave background observations. Adapting existing constraints on the annihilation cross section of dark matter particles [45] by equating the energy injection rates in the annihilation and decay processes at $z = 1091$, we find $\tau \gtrsim 2\ \mathrm{Myr}\,[\mathrm{TeV}/m_X][2\Omega_{\tilde{G}^*}/\Omega_{\mathrm{DM}}][\Delta E/3.5\ \mathrm{keV}]$.

VII. RESULTS

We now have all the ingredients to identify viable example models and their observational implications.

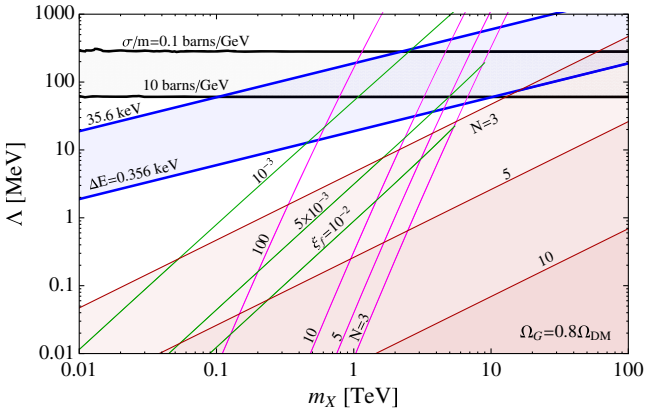

FIG. 1 (color online). Thermal strongly interacting dark matter with $\Omega_G = 0.8\Omega_{\mathrm{DM}}$ and $\Omega_{\tilde{g}} = 0.2\Omega_{\mathrm{DM}}$. For fixed (m_X, Λ), N and ξ_f are determined by the relic densities; contours of $N = 3, 5, 10, 100$ and $\xi_f = 10^{-3}, 5\times 10^{-3}, 10^{-2}$ are shown. In the indicated bands, $\sigma/m = 0.1$–$10\ \mathrm{barn/GeV}$ and $\Delta E = 0.356$–35.6 keV. Where these overlap, the model may explain both self-interactions and the 3.5 keV line through long-lifetime $\tilde{G}^*$ decays (see text). In the lower-right shaded regions, $\tilde{G}$ reannihilation may be significant for the values of N indicated.

We begin by considering a completely thermal scenario, in which the gluino and glueball relic densities are given by Eqs. (3) and (5). As an example, we consider the case with $\Omega_G = 0.8\Omega_{\mathrm{DM}}$ and $\Omega_{\tilde{g}} = 0.2\Omega_{\mathrm{DM}}$. The required values of N and ξ_f are shown in the (m_X, Λ) plane in Fig. 1. Relatively cold hidden sectors are required to avoid glueballs overclosing the Universe.

In this glueball-dominated scenario, the self-interaction cross section is essentially σ_G, and so is in the desired range for $\Lambda \sim 100$ MeV. This constraint and the $\Delta E = 3.56$ keV band are also shown in Fig. 1. These bands overlap, for example, at $(m_X, \Lambda) = (3\ \mathrm{TeV}, 70\ \mathrm{MeV})$, where $\alpha_X \approx 0.013$, $N \approx 10$, and $\xi_f \approx 4\times 10^{-3}$. At this point, $\sigma_{\tilde{G}^*}$ is far too small to explain the keV line flux in the short-lifetime scenario. However, the flux can be explained by long-lifetime decays. Equation (14) implies $\tau \sim 30$ Gyr, which, given Eq. (10), implies a connector mass $m_C \sim 4$–6 TeV.

We now consider the case where the gluon density is depleted to $\Omega_G \approx 0$ through some mechanism, such as the one of Ref. [25] described above. Glueballs then do not overclose the Universe for any ξ_f, and we consider $\xi_f = 1$. The resulting parameters are shown in Fig. 2.

In this pure $\tilde{G}$ scenario, the preferred self-interactions and keV line energy overlap, for example, at $(m_X, \Lambda) = (350\ \mathrm{GeV}, 20\ \mathrm{MeV})$, where $\alpha_X \approx 0.019$ and $N \approx 10$. The keV line flux may again be explained by long-lifetime decays; in this case, Eq. (14) implies $\tau \sim 1000$ Gyr, which, given Eq. (10), implies $m_C \sim 3$–9 TeV. In this case, however, the self-interactions also imply a large up-scattering rate, and so the short-lifetime scenario is also viable where all three bands overlap in Fig. 2. A lifetime of $\tau \sim 10^{15}$ s

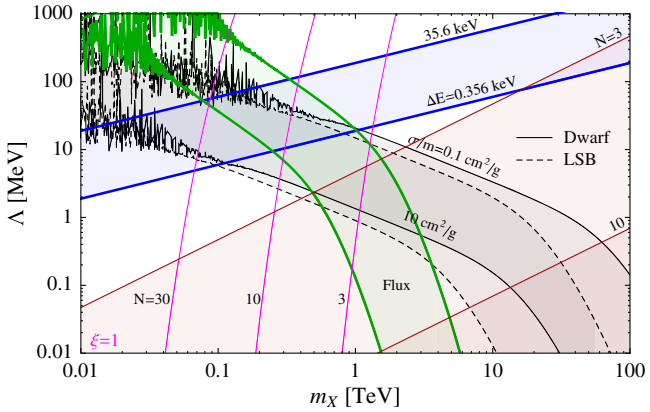

FIG. 2 (color online). Pure glueballino strongly interacting dark matter with $\xi_f = 1$. For fixed (m_X, Λ), N is determined by $\Omega_{\tilde{g}} = \Omega_{\rm DM}$; contours of $N = 3, 10, 30$ are shown. In the indicated bands, $\sigma/m = 0.1$–10 barn/GeV, $\Delta E = 0.356$–35.6 keV, and short-lifetime $\tilde{G}^*$ decays give a keV line flux within an order of magnitude to explain the Perseus observations, assuming $\sigma_{\tilde{G}^*} = \sigma_{\tilde{G}}$. The flux may also be explained by long-lifetime $\tilde{G}^*$ decays (see text). In the lower-right shaded regions, $\tilde{G}$ reannihilation may be significant for the values of N indicated.

implies $m_C \sim 500$–700 GeV, which is beyond collider limits on particles that have electric charge, but not strong interactions, in the visible sector.

VIII. CONCLUSIONS

Currently there are tantalizing astrophysical indications that dark matter may be self-interacting and the source of a 3.5 keV x-ray line. Although neither of the indications for self-interactions and keV lines is unambiguously compelling individually, they are both interesting, and more so if they may be explained simultaneously in a simple model.

We have explored these in the context of a simple hidden sector: a supersymmetric pure SU(N) gauge theory. The astrophysical hints favor $m_X \sim$ TeV thermal relics interacting with $\Lambda \sim 100$ MeV force carriers, with photons created by transitions between highly degenerate states with $\Delta E \sim 10$ keV. In this model, the qualitative hierarchy $\Delta E \ll \Lambda \ll m_X$ and the quantitative relation $\Delta E m_X \sim \Lambda^2$ are naturally explained by asymptotic freedom and, essentially, atomic physics. Despite its simple formulation, the model has a rich cosmology, with both glueballs and glueballinos contributing to dark matter, and decays that can be either short and long compared to the age of the Universe. The short-lifetime possibility is remarkable in that the desired self-interactions imply a keV line flux roughly in accord with observations, albeit with some tension between the various data sets, while the long-lifetime scenario provides a beautifully consistent explanation for the x-ray line observed in clusters of galaxies, M31, and MW observations.

ACKNOWLEDGMENTS

We are grateful to Geoff Bodwin for helpful correspondence. J. L. F. and Y. S. thank the CERN Theoretical Physics Group and J. L. F. thanks the Technion Particle Physics Center for hospitality. This research is supported in part by BSF Grant No. 2010221 (J. L. F. and Y. S.), NSF Grants No. HY–1316792 (J. L. F. and T. M. P. T.), No. PHY–1214648, and No. PHY–1316792 (M. K.), ISF Grant No. 1367/11 and the ICORE Program of Planning and Budgeting Committee and ISF Grant No. 1937/12 (Y. S.), DOE Grant No. DE-SC0011632 and the Gordon and Betty Moore Foundation through Grant No. 776 (K. B.), a Guggenheim Foundation grant (J. L. F.), and the University of California, Irvine, through a Chancellor's Fellowship (T. M. P. T.).

[1] P. Ade *et al.* (Planck Collaboration), arXiv:1303.5076 [Astron. Astrophys. (to be published)].
[2] M. Rocha, A. H. G. Peter, J. S. Bullock, M. Kaplinghat, S. Garrison-Kimmel, J. Oñorbe, and L. A. Moustakas, Mon. Not. R. Astron. Soc. **430**, 81 (2013).
[3] A. H. G. Peter, M. Rocha, J. S. Bullock, and M. Kaplinghat, Mon. Not. R. Astron. Soc. **430**, 105 (2013).
[4] M. Vogelsberger, J. Zavala, and A. Loeb, Mon. Not. R. Astron. Soc. **423**, 3740 (2012).
[5] J. Zavala, M. Vogelsberger, and M. G. Walker, Mon. Not. R. Astron. Soc. **431**, L20 (2013).
[6] E. Bulbul, M. Markevitch, A. Foster, R. K. Smith, M. Loewenstein, and S. W. Randall, Astrophys. J. **789**, 13 (2014).
[7] A. Boyarsky, O. Ruchayskiy, D. Iakubovskyi, and J. Franse, Phys. Rev. Lett. **113**, LP14378 (2014).
[8] I. Y. Kobsarev, L. B. Okun, and I. Y. Pomeranchuk, Sov. J. Nucl. Phys. **3**, 837 (1966).
[9] J. L. Feng and J. Kumar, Phys. Rev. Lett. **101**, 231301 (2008).
[10] J. L. Feng, H. Tu, and H.-B. Yu, J. Cosmol. Astropart. Phys. 10 (2008) 043.
[11] J. L. Feng and Y. Shadmi, Phys. Rev. D **83**, 095011 (2011).
[12] J. L. Feng, V. Rentala, and Z. Surujon, Phys. Rev. D **84**, 095033 (2011).
[13] J. L. Feng, V. Rentala, and Z. Surujon, Phys. Rev. D **85**, 055003 (2012).
[14] J. Kang, M. A. Luty, and S. Nasri, J. High Energy Phys. 09 (2008) 086.
[15] G. D. Kribs, T. S. Roy, J. Terning, and K. M. Zurek, Phys. Rev. D **81**, 095001 (2010).

[16] D. S. Alves, S. R. Behbahani, P. Schuster, and J. G. Wacker, Phys. Lett. B **692**, 323 (2010).
[17] A. Falkowski, J. Juknevich, and J. Shelton, arXiv: 0908.1790.
[18] M. Lisanti and J. G. Wacker, Phys. Rev. D **82**, 055023 (2010).
[19] D. Spier Moreira Alves, S. R. Behbahani, P. Schuster, and J. G. Wacker, J. High Energy Phys. 06 (2010) 113.
[20] K. Kumar, A. Menon, and T. M. Tait, J. High Energy Phys. 02 (2012) 131.
[21] T. Higaki, K. S. Jeong, and F. Takahashi, J. Cosmol. Astropart. Phys. 08 (2013) 031.
[22] M. Heikinheimo, A. Racioppi, M. Raidal, C. Spethmann, and K. Tuominen, Mod. Phys. Lett. A **29**, 1450077 (2014).
[23] Y. Bai and P. Schwaller, Phys. Rev. D **89**, 063522 (2014).
[24] J. M. Cline, Z. Liu, G. D. Moore, and W. Xue, Phys. Rev. D **90**, 015023 (2014).
[25] K. K. Boddy, J. L. Feng, M. Kaplinghat, and T. M. P. Tait, Phys. Rev. D **89**, 115017 (2014).
[26] Y. Hochberg, E. Kuflik, T. Volansky, and J. G. Wacker, Phys. Rev. Lett. **113**, 171301 (2014).
[27] J. M. Cline and A. R. Frey, J. Cosmol. Astropart. Phys. 10 (2014) 10.
[28] J. E. Juknevich, D. Melnikov, M. J. Strassler, J. High Energy Phys. 07 (2009) 55.
[29] E. D. Carlson, M. E. Machacek, and L. J. Hall, Astrophys. J. **398**, 43 (1992).
[30] M. S. Chanowitz and S. R. Sharpe, Phys. Lett. **126B**, 225 (1983).
[31] R. Dowdall, C. Davies, T. Hammant, and R. Horgan, Phys. Rev. D **86**, 094510 (2012).
[32] A. Boyarsky, J. Franse, D. Iakubovskyi, and O. Ruchayskiy, arXiv:1408.2503.
[33] S. Riemer-Sorensen, arXiv:1405.7943.
[34] T. E. Jeltema and S. Profumo, arXiv:1408.1699.
[35] D. Malyshev, A. Neronov, and D. Eckert, Phys. Rev. D **90**, 103506 (2014).
[36] M. E. Anderson, E. Churazov, and J. N. Bregman, arXiv: 1408.4115.
[37] A. Boyarsky, J. Franse, D. Iakubovskyi, and O. Ruchayskiy, arXiv:1408.4388.
[38] E. Dudas, L. Heurtier, and Y. Mambrini, Phys. Rev. D **90**, 035002 (2014).
[39] J. M. Cline, Y. Farzan, Z. Liu, G. D. Moore, and W. Xue, Phys. Rev. D **89**, 121302 (2014).
[40] D. P. Finkbeiner and N. Weiner, arXiv:1402.6671.
[41] M. T. Frandsen, F. Sannino, I. M. Shoemaker, and O. Svendsen, J. Cosmol. Astropart. Phys. 05 (2014) 033.
[42] J. M. Cline, Z. Liu, G. Moore, and W. Xue, Phys. Rev. D **89**, 043514 (2014).
[43] M. Kaplinghat, R. E. Keeley, T. Linden, and H.-B. Yu, Phys. Rev. Lett. **113**, 021302 (2014).
[44] L. E. Strigari, J. S. Bullock, M. Kaplinghat, J. D. Simon, M. Geha, B. Willman, and M. G. Walker, Nature (London) **454**, 1096 (2008).
[45] S. Galli, F. Iocco, G. Bertone, and A. Melchiorri, Phys. Rev. D **84**, 027302 (2011).